Precision of morphogen-driven tissue patterning during development is enhanced through contact-mediated cellular interactions

Chandrashekar Kuyyamudi,[1,2] Shakti N. Menon,[1] and Sitabhra Sinha[1,2]
[1]*The Institute of Mathematical Sciences, CIT Campus, Taramani, Chennai 600113, India*
[2]*Homi Bhabha National Institute, Anushaktinagar, Mumbai 400 094, India*

(Received 16 November 2021; accepted 30 January 2023; published 13 February 2023)

Cells in developing embryos reliably differentiate to attain location-specific fates, despite fluctuations in morphogen concentrations that provide positional information and in molecular processes that interpret it. We show that local contact-mediated cell-cell interactions utilize inherent asymmetry in the response of patterning genes to the global morphogen signal yielding a bimodal response. This results in robust developmental outcomes with a consistent identity for the dominant gene at each cell, substantially reducing the uncertainty in the location of boundaries between distinct fates.

DOI: 10.1103/PhysRevE.107.024407

I. INTRODUCTION

The ubiquity of noise in nature requires that biological processes be robust to it [1,2]. In particular, during development, small deviations resulting from chance events at earlier stages can get amplified over time leading to pathological outcomes [3,4]. Nevertheless, embryos exhibit a highly reproducible sequence of cellular division, differentiation, and rearrangement resulting in consistent physiological organizations [5–8]. Such pattern formation [9,10] during morphogenesis involves cells adopting distinct roles (fates) via differential gene expression [11]. Fates are determined by the positional information provided by the local concentration of *morphogen* molecules diffusing from localized sources [Fig. 1(a)]. Pattern formation of this nature, which is guided by a global field (in this case, the morphogen gradient), is referred to as *boundary-organized* to distinguish it from self-organized pattern formation mechanisms such as that suggested by Turing in the context of reaction-diffusion systems [12–15]. The domains of distinct fates are characterized by sharp boundaries [16] whose locations are invariant for a species, e.g., between cells expressing dorsal and ventral fates in a *Xenopus* embryo [Fig. 1(b)] [4]. This occurs despite the ubiquity of noise, which can have sources that are intrinsic (such as transcriptional bursts) or extrinsic, resulting in cells exhibiting variability that cannot be attributed to any genetic differences [2,17,18]. For example, fluctuations in the morphogen concentration can arise due to stochasticity in the synthesis, degradation and diffusive transport of molecules [Fig. 1(a), inset] [14,19–21]. In addition, the steps involved in the intra-cellular response are inherently noisy, as the underlying probabilistic processes involve a small number of molecules [22–24].

In the absence of an explicit mechanism for noise reduction, cell fates in a model system can exhibit a high degree of variation [Fig. 1(c)]. Comparable expression levels of patterning genes in a number of cells suggest that the resulting fates are primarily decided by random chance events [25,26]. Hence, instead of a highly reproducible spatial pattern characterized by precisely located fate boundaries, the length of the different fate domains would have varied considerably across realizations [Fig. 1(d)]. Mechanisms that could be operating *in vivo* to reduce this variability [27,28] could involve, e.g., self-enhanced morphogen degradation, pre-steady-state interpretation of the gradient, stochastic focusing and negative feedback in genetic regulatory networks [14,28–32]. Cell fate consistency can also be promoted by processes that reduce fluctuations in the morphogen concentration gradient [26,33–35]. In general, all such mechanisms that improve the reliability of cell fate decisions based on spatial location, effectively pool together information from multiple measurements of the local morphogen signal [6]. While a single cell may achieve this by temporal integration of the signal, an alternative is for neighboring cells to share information [36]. As cells in the developing embryo can communicate with those in close proximity through contact-mediated signaling, such interactions can be a possible mechanism for spatial integration of the morphogen signal [6,37]. A notable example is the evolutionarily conserved notch signaling pathway [38–41], known to play a fundamental role in all metazoan development [38,42,43]. It is triggered when notch receptors on a cell surface bind to membrane-bound proteins (e.g., Delta or Jagged ligands) of a neighboring cell. Although it has been suggested that such contact-mediated signaling may regulate noise [6,44,45], an explicit mechanism for this is yet to be established.

In this paper we demonstrate that cells can act in concert to attenuate the impact of noise, thereby enhancing the precision of the boundary demarcating distinct fates. Specifically, we investigate how intercellular signaling regulates the expression of mutually inhibiting patterning genes (A, B) that determine the developmental fate of a cell. We observe a remarkable decrease in cell fate uncertainty near the boundary between the two domains if the downstream effector S

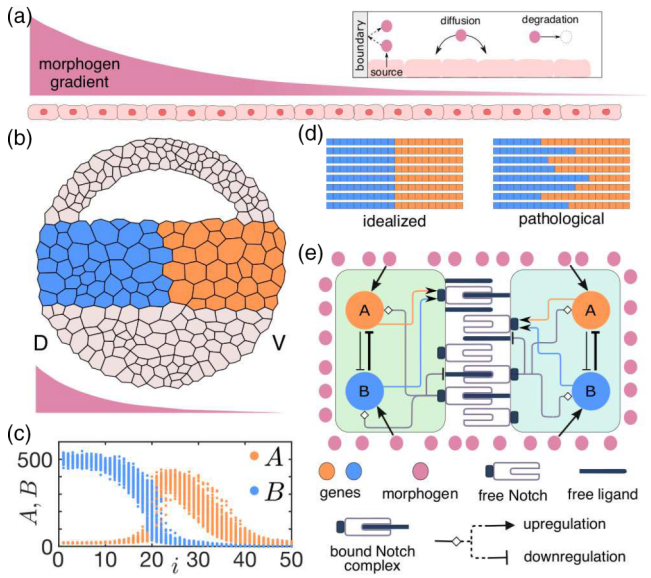

FIG. 1. Cell fate determination through a morphogen concentration gradient needs to be robust against stochastic fluctuations. (a) A morphogen gradient across a cellular array results from the processes (shown in the inset) of secretion of molecules from a source located at the boundary of the domain, their diffusion across space, and degradation over time such that the decay rate is linearly proportional to its concentration. (b) Schematic representation of a *Xenopus* embryo where the differentiation of the cells of the mesoderm into dorsal and ventral fates (represented by blue and orange, respectively) is guided by the concentration gradient of the morphogen *activin* between the dorsal (D) and ventral (V) ends (displayed below the embryo). (c) The steady-state expression of patterning genes A, B across a 1D array comprising N cells, with the indices of the cells indicated by $i = 1, \ldots, N(= 50)$, subject to a noisy morphogen gradient in the absence of interaction between the cells. Results of 300 different realizations are shown. (d) While in the absence of noise the boundary separating the regions with the two different fates corresponding to $B > A$ (blue) and $A > B$ (orange) is expected to occur at the same position across all realizations (the idealized situation shown at left), fluctuations in the morphogen concentration and gene expression dynamics results in variations across realizations (shown at right) if fate determination occurs only on the basis of positional information provided by the morphogen gradient. (e) Interactions between neighboring cells mediated by the notch signaling pathway (shown here schematically) can aid in the robust determination of fate boundaries in the presence of noise. Genes A and B comprising the morphogen interpretation module affect the expression of genes coding for notch receptors. The notch intracellular domain (NICD), released from the bound notch complex that results from the *trans*-activation of notch receptors, in turn up- or downregulates the expression of A and B (depending on the type of interaction).

of the notch signaling pathway upregulates the patterning gene A that expresses at a lower morphogen concentration, or equivalently, downregulates the other gene B. Insight into the process by which the coupling counters noise is provided by the observation that robustness requires the timescale of the contact-induced signal to be longer than those associated with gene expression dynamics. This effectively allows spatial integration of the information provided by the morphogen around the local neighborhood of each cell, thereby attenuating noise. Our results show that intercellular notch signaling can exploit inherent asymmetries in the interactions between patterning genes and their response to the morphogen, yielding a highly robust developmental outcome.

II. MODEL

To investigate the potential role of contact-mediated interactions in generating spatial patterns of cell fates that are robust to stochastic fluctuations, we consider a linear array of cells exposed to a morphogen concentration gradient. The morphogen molecules are secreted at a constant rate α_M from one end of the array and have a mean lifetime τ_M. They randomly disperse in the medium with diffusion coefficient D_M, resulting in fluctuations of their concentration around an exponentially decaying spatial profile. The temporally averaged signal strength sensed by a cell at a distance x away from the source is $M(x) = M(0)\exp(-x/\lambda_M)$, where λ_M is the characteristic length scale of the gradient. The signal governs the differential expression of genes comprising the morphogen interpretation module. We consider the simplest module yielding spatial patterns which comprises two genes, A and B [Fig. 1(e)], such as *Goosecoid* and *Brachyury* involved in mesodermal patterning in *Xenopus* induced by the morphogen *activin* [46,47]. This framework is also applicable to other examples involving two patterning genes whose differential expression is induced by the local morphogen concentration, such as the genes *orthodenticle* and *hunchback* responding to a gradient in Bicoid concentration, and the genes *twist* and *rhomboid* induced by graded Dorsal activity, that are required to establish anteroposterior polarity and the dorsoventral axis, respectively, in the developing *Drosophila* embryo [48].

As is characteristic of gene circuits that respond to an external morphogen concentration, the two patterning genes are assumed to mutually repress each other [14,48–50]. The maximally expressed gene in a cell decides its fate. As mentioned earlier, compared to gene B, gene A is expressed at a relatively lower morphogen concentration. Asymmetric mutual repression such that B inhibits A more strongly than A does B. ensures that B expression is favored at higher morphogen concentrations, preventing a homogeneous fate for the entire domain.

When both A and B are expressed at high levels, the gene encoding notch is upregulated, resulting in increased concentration of free receptors (R). This enhances the strength of intercellular coupling by increasing the probability of binding to ligands of a neighboring cell. Such *trans*-activation of notch receptors leads to a signaling cascade having a downstream effector S that regulates the patterning gene expression. Based on whether S up or downregulates the expression of gene A or gene B, we can classify the intercellular interactions into four different types. We report below in detail the dynamical consequences of each type of coupling. The signaling resulting from *trans*-activation of notch receptors also results in the repression of the production of ligand protein [39,51], thereby decreasing the concentration of free ligands (L).

TABLE I. Functions and parameters defining different types of intercellular signaling. The classification is based upon the nature of interaction, viz., upregulation (→) or downregulation (⊣), and the identity of the patterning gene whose expression is regulated by the notch downstream effector S, i.e., A or B.

	Φ_A	Φ_B	γ_A	γ_B
$S \dashv B$	1	$Q^g/Q^g + S^g$	0	0
$S \rightarrow A$	1	1	>0	0
$S \dashv A$	$Q^g/Q^g + S^g$	1	0	0
$S \rightarrow B$	1	1	0	>0

The equations describing the stochastic dynamics of all variables $\mathbf{X} : \{M, A, B, R, L, S\}$ in our model have the form $d\mathbf{X} = \mathcal{F}_\mathbf{X} dt + \mathcal{G}_\mathbf{X} dW$, with the stochastic component being $\mathcal{G}_\mathbf{X} = \eta_\mathbf{X}\mathbf{X}$ where $\eta_\mathbf{X}$ are the noise strengths associated with the different variables and dW is a Wiener process [52,53]. The deterministic component $\mathcal{F}$ for the system variables are given by

$$\mathcal{F}_M = \alpha_M \delta_{i,1} - D_M \nabla^2 M - \frac{M}{\tau_M},$$

$$\mathcal{F}_A = \alpha_A \mathcal{H}_h(M, K_1)\mathcal{H}'_h(B, K_3)\Phi_A + \gamma_A \mathcal{H}_g(S, Q) - \frac{A}{\tau_A},$$

$$\mathcal{F}_B = \alpha_B \mathcal{H}_h(M, K_2)\mathcal{H}'_h(A, K_4)\Phi_B + \gamma_B \mathcal{H}_g(S, Q) - \frac{B}{\tau_B},$$

$$\mathcal{F}_R = \beta_{R_0} + \beta_R \mathcal{H}_g(A, J)\mathcal{H}_g(B, J) - k_{\rm tr} R L_{\rm tr} - \frac{R}{\tau_R},$$

$$\mathcal{F}_L = \beta_{L_0} + \beta_L \mathcal{H}'_g(S, K_5) - k_{\rm tr} R_{\rm tr} L - \frac{L}{\tau_L},$$

$$\mathcal{F}_S = k_{\rm tr} R L_{\rm tr} - \frac{S}{\tau_S},$$

where $R_{\rm tr} (= \sum_{i\in\mathcal{N}} R_i)$ and $L_{\rm tr} (= \sum_{i\in\mathcal{N}} L_i)$ are the total concentrations of receptors and ligands, respectively, in the neighboring cell(s) ($\mathcal{N}$ denoting this set). The noise strengths for the morphogen and patterning genes in the coupled system are same as that for the uncoupled system, viz., $\eta_M = 1$, $\eta_A = \eta_B = 0.1$. For simplicity it is assumed that the notch receptor, ligand, and downstream effector molecules have the same noise strength $\eta (= 0.01)$. The coupling enhanced precision of the fate boundary is seen to be invariant over a large range of η [54]. The Hill functions corresponding to activation and inactivation of X are $\mathcal{H}_z(X, C) = X^z/(C^z + X^z)$ and $\mathcal{H}'_z(X, C) = C^z/(C^z + X^z)$, respectively, with C as the half-saturation constant and z being the Hill exponent. The functions $\Phi_{A,B} = Q^g/(Q^g + S^g)$, if S inactivates the corresponding gene A or B, respectively, and $= 1$, otherwise. The coefficients $\gamma_{A,B}$ of the Hill functions that quantify the signal's contribution to the expression of patterning genes is >0 if S activates the corresponding gene, and $= 0$, otherwise. Together they characterize the four distinct types of intercellular interactions defined in Table I. To quantitatively characterize the role of intercellular interaction in promoting robustness to noise, we compare the variance of the spatial location of the fate boundary when the cells interact via notch signaling, with the case when the cells attain their fates independent of their neighbors. Figure 1(c) displays the spatial distribution of steady-state values of A and B when the cells are uncoupled. In cells near the fate boundary (i.e., $i \sim 20$), the expression of both genes varies over a large range, with substantial overlap between the two distributions. As a result, cell fates vary across realizations [Fig. 1(d), right], indicative of insufficient positional information to conclusively determine the eventual identities. Such ambiguity can lead to a biologically undesirable outcome, viz., high variability in embryonic patterning [55,56].

The strength of the interaction between notch signaling and patterning gene expression dynamics is regulated in our model by the half-saturation constants Q and J, as well as K_5, which controls the strength of repression of ligand expression by the notch signal (see the expressions for $\mathcal{F}_{A,B}$, $\mathcal{F}_R$, and $\mathcal{F}_L$, respectively, defined above). We focus on (i) Q, the magnitude of S above which the signal noticeably affects patterning gene expression, and (ii) J, which determines the expression levels of the patterning genes above which production of notch receptors is appreciably increased. As the coupling-induced suppression of noise occurs even when S has no effect on L production, we may conclude that the phenomenon is not critically dependent on the value of K_5. Two additional parameters γ_A and γ_B also play a role but only when the signal S *upregulates* the patterning genes.

III. RESULTS

Figure 2 shows the dispersion in the fate boundary position in a system of N coupled cells upon varying Q and J over a large range. While for all four types of interactions we observe a substantial reduction in the extent to which the location l_B of the fate boundary fluctuates across realizations, this is most prominent when the interaction involves either S downregulating the expression of B [Fig. 2(a)], or equivalently, upregulating the expression of its inhibitor A [Fig. 2(b)]. For these two types of interactions, we observe not only a much larger area of the (Q, J) parameter space where the variance $\sigma^2(l_B)$ is lower than that in the absence of intercellular interactions, but also a relatively greater certainty in the location of the boundary between the different fates. We note that alternative measures of robustness yield qualitatively similar results (see Figs. S1 and S2 [54]).

For the type of interaction in which the signal downregulates A (or equivalently, upregulates B), the function Φ_A, and hence the production term in $\mathcal{F}_A$, decreases to very low values for large S. As a result, B is favored to dominate over A in the region where the patterning genes are expressed at comparable levels when the cells are uncoupled. This would lead one to expect an analogous situation to that in which S downregulates B expression, but with B replacing A as the preferred cell fate around the fate boundary location for the noninteracting case. However, as this region is located relatively far from the morphogen source, the local concentration of M may not be high enough to promote the expression of B while being sufficient for the expression of A (as $K_2 > K_1$). As a result, the advantage conferred to B by the contact-mediated interaction is offset by the low morphogen concentration that favors A, preventing outright dominance by either gene in this region. Hence, these two types of interactions between S and the patterning genes are unable

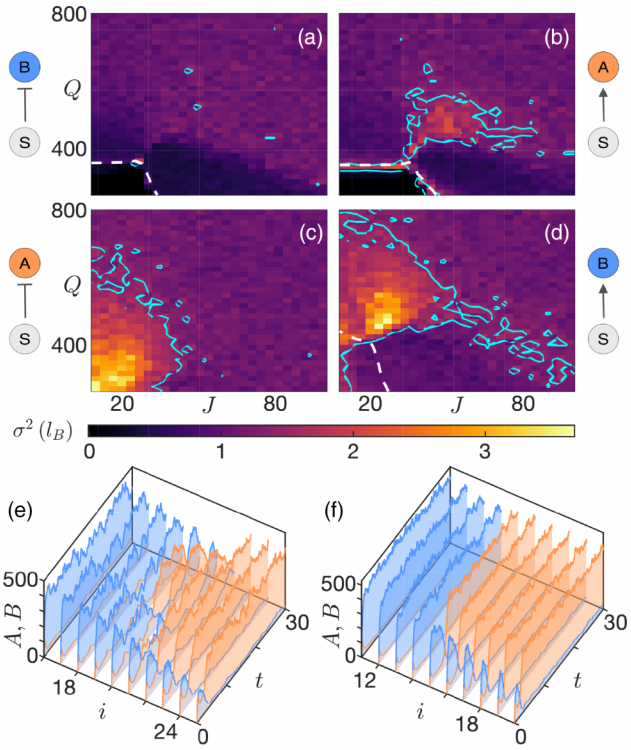

FIG. 2. Robust determination of cell fates results from interaction between stochastic gene expression dynamics and contact-mediated signaling. The intercellular interactions mediated by the notch downstream signal (S) can be classified into four types, determined by which of the patterning genes (A or B) is up/downregulated by S, as represented by the motifs shown beside each panel (a)–(d) [arrows as in Fig. 1(e)]. For each type, the spatial pattern formed by cells adopting distinct fates A, B in a 1D domain comprising $N(= 50)$ cells subject to a morphogen gradient is characterized by the location l_B of the boundary [$\sim$20, in absence of any interactions between the cells, see Fig. 1(c)] demarcating the segments expressing the two fates. The variance in l_B across 300 stochastic realizations is shown for each choice of the pair of parameters quantifying the strength of intercellular coupling, viz., J representing critical value of patterning gene expression segregating low/high receptor production and Q representing critical signal intensity that distinguishes between weak and strong regulation of patterning gene expression. The continuous curves in each panel are contours indicating the variance in l_B in the absence of intercellular interactions ($\simeq 1.38$). The regions in the J-Q plane above the broken curves (shown in white) correspond to the mean value of l_B lying within [10,30], i.e., 50% of its value in the uncoupled case. Note that, for coupling types in which S upregulates A either directly (b), or indirectly via suppression of its inhibitor B (a), fluctuations in l_B are markedly reduced over a wider range of J and Q. (e, f) Temporal evolution of the expression of A and B shown for cells around l_B for the uncoupled case, contrasting (e) the dynamics seen in absence of any intercellular interactions, with (f) that obtained when S inhibits B [as in panel (a)]. While the uncoupled cells exhibit large fluctuations in expression levels with uncertainty in l_B sustained for a long time, in the presence of intercellular interactions cells rapidly converge to their eventual fates.

to reduce the variability in fate boundary position for a wide range of choices of the parameters Q and P [see Figs. 2(c) and 2(d)].

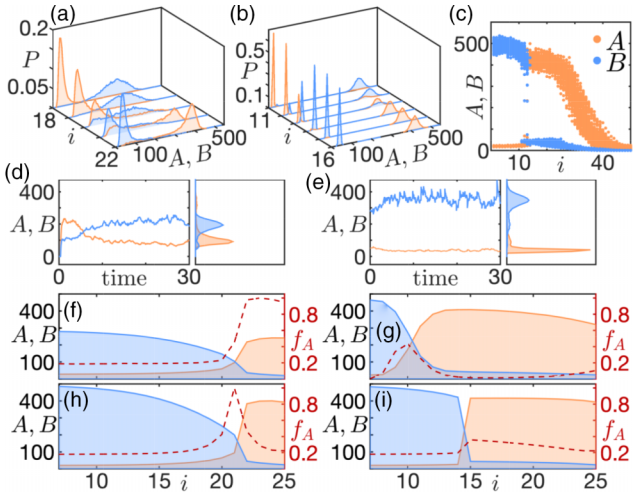

FIG. 3. Reduction in variability of response to fluctuating morphogen concentrations by contact-mediated signaling. (a), (b) Steady-state distributions for the expression levels of the patterning genes A and B shown for cells located around the respective positions of the fate boundary when (a) intercellular interactions are absent, or (b) the notch downstream signal S suppresses expression of B [as in Fig. 2(a)]. In the uncoupled case, the distributions are extremely broad with a high degree of overlap close to the fate boundary. Interactions, on the other hand, result in sharply defined peaks at very low and high values, with the dominant gene at a given cell clearly identifiable. This leads to a steady-state expression of the patterning genes [shown in panel (c) for a 1D array of 50 cells] that exhibits a robust, sharply defined cell fate boundary (at $i \approx 12$) even in the presence of a noisy morphogen gradient. Results of 300 different realizations are shown. (d), (e) Time-series (left) and corresponding distributions (right) of patterning gene expressions for a cell placed in a morphogen gradient when it is (d) isolated or (e) coupled to a neighboring cell. The coupling-induced separation of A, B reduces the uncertainty in fate determination. (f)–(i) The numerical results (f, uncoupled; g, coupled) are supported by analytical calculations for a pair of coupled cells using linear noise approximation where the high degree of uncertainty as measured by the normalized Fano factor f_A (broken curve) in the absence of coupling (h) decreases markedly on including contact-mediated signaling between the cells (i). Shaded regions represent the position-dependent steady-state expression levels for A and B.

To explain this enhanced robustness when S suppresses the patterning gene B (or equivalently, promotes A), we note that this suppression occurs specifically in the region ($i \geqslant 13$) where, in the absence of coupling, A, B are expressed at comparably high levels ($> J$) in the steady state and where the two distributions consequently overlap [Fig. 3(a)]. The notch-mediated interaction leads to the dominance of A over B in this region consistently across all realizations [Fig. 3(b)]. For cells closer to the morphogen source ($i \leqslant 12$), B dominates because of the asymmetric mutual repression between the patterning genes, resulting in low expression levels of A and consequently, negligible production of S. The intercellular interactions can, thus, be seen as enhancing the distinction between the steady-state levels of A and B, leading to a sharply defined fate boundary [Fig. 3(c), compare with Fig. 1(c)]. Note that the boundary shifts closer to the morphogen source (with respect to its location in the uncoupled

case), as the suppression of B by S favors the dominance of A in regions where the two genes would have had similar expression levels in the absence of interactions. Consistent with this explanation, the reverse is observed for types of interactions where S instead suppresses A (or promotes B) with the fate boundary location moving further away from the morphogen source (as shown in Fig. S3 [54]). Our model, thus, helps explain the shift in fate boundary that has been observed when cells communicate via notch signaling [57,58].

The mechanism by which intercellular coupling reduces the uncertainty in fate specification can be clarified by considering a pair of cells that are located at adjacent positions along the morphogen gradient. As seen in Figs. 3(d) and 3(e), coupling leads to an increased separation between the expression levels of A and B. By analytically obtaining the variance in the gene expression levels of this reduced system [59], we can explicitly reproduce the reduction in uncertainty (most apparent at the cell fate boundary) arising from contact-mediated signaling [Figs. 3(f) and 3(g)]. This is quantified in terms of the Fano factor F for the expression level X of a patterning gene and is defined as

$$F_X = \frac{\langle X^2 \rangle - \langle X \rangle^2}{\langle X \rangle}, \tag{1}$$

where $\langle \dots \rangle$ represents the temporal average. For ease of comparison between the analytical and numerical results in presence and absence of intercellular coupling, we normalize the factor by its maximum value in the uncoupled case, viz., $f = F/F^{\max}_{\text{uncoupled}}$. We formulate the mass-action kinetics in terms of stoichiometric coefficients and propensities, by considering the concentrations in of the various chemical species $\mathbf{X} : \{M, A, B, R, L, S\}$ undergoing single-step reactions for each of the cells in the system being considered. This yields a stoichiometric matrix, whose elements are then used to construct a diffusion matrix $\mathbf{D}$ that occurs in the matrix equation

$$\mathbf{J}\Sigma + \Sigma\mathbf{J}^T = -\mathbf{D}, \tag{2}$$

where $\mathbf{J}$ is the Jacobian calculated for the fixed point of the corresponding deterministic system. Solving this equation we obtain the stationary covariance matrix Σ, thereby obtaining the variance of the expression levels that is used to calculate the Fano factor. Details of calculations, including complete set of codes, are available at Ref. [60]. The results obtained are shown in Figs. 3(h) and 3(i) in terms of the normalized Fano factor f_A for the expression level in one of the cells. We also note that independent of the mean morphogen concentration M (and hence, the cell's position in the array [61,62]), the gene expression level is robust to noise over a range of τ_S.

IV. CONCLUSION

To conclude, we have shown that contact-mediated interaction between cells can reduce the uncertainty in cell fates that arise from both stochastic fluctuations in the morphogen concentration and intrinsic noise. Even though the signaling mechanism we employ is also subject to random variability in its components, it is able to markedly reduce the variability in the position of the boundary between regions expressing distinct cell fates. This enhanced robustness suggests a functional role for the higher expression level of notch, e.g., at the boundary between the regions expressing dorsal and ventral fates in the *Drosophila* hindgut [63], and in the boundaries of the organ of corti in the mice cochlea [64]. A direct experimental test of our model can involve verifying that notch activity is stronger in those differentiating cells that would have comparable levels of expression for different patterning genes in absence of notch. The results reported here show that the nature of interaction between the downstream effector of the intercellular signaling mechanism and the patterning gene(s) is important in determining the extent to which coupling between cells enhance the robustness of cell fate patterns. An experimentally verifiable consequence is that the mechanism described here is more effective in suppressing noise and reducing variability when notch signaling upregulates the patterning gene that requires a relatively lower concentration of the morphogen to be expressed (or equivalently, downregulates the gene repressing it).

ACKNOWLEDGMENTS

We thank Marcin Zagórski for helpful discussions. S.N.M. has been supported by the IMSc Complex Systems Project (12th Plan), and the Center of Excellence in Complex Systems and Data Science, both funded by the Department of Atomic Energy, Government of India. The simulations required for this work were supported by IMSc High Performance Computing facility (hpc.imsc.res.in) [Nandadevi].

[1] H. Kitano, Nat. Rev. Genet. **5**, 826 (2004).
[2] L. S. Tsimring, Rep. Prog. Phys. **77**, 026601 (2014).
[3] C. H. Waddington, *The Strategy of the Genes* (George Allen & Unwin, London, UK, 1957).
[4] L. Wolpert, C. Tickle, and A. M. Arias, *Principles of Development* (Oxford University Press, New York, NY, 2015).
[5] P. W. Sternberg, Science **303**, 637 (2004).
[6] A. D. Lander, Science **339**, 923 (2013).
[7] S. Gilbert, *Developmental Biology* (Sinauer, Sunderland, MA, 2013).
[8] M.-A. Félix and M. Barkoulas, Nat. Rev. Genet. **16**, 483 (2015).
[9] M. C. Cross and P. C. Hohenberg, Rev. Mod. Phys. **65**, 851 (1993).
[10] A. J. Koch and H. Meinhardt, Rev. Mod. Phys. **66**, 1481 (1994).
[11] S. Huang, G. Eichler, Yaneer Bar-Yam, and D. E. Ingber, Phys. Rev. Lett. **94**, 128701 (2005).
[12] L. Wolpert, J. Theor. Biol. **25**, 1 (1969).
[13] L. Wolpert, Development **107**, 3 (1989).
[14] J. B. Gurdon and P.-Y. Bourillot, Nature (London) **413**, 797 (2001).
[15] J. Sharpe, Development **146**, dev185967 (2019).
[16] S. B. Cambridge, R. L. Davis, and J. S. Minden, Science **277**, 825 (1997).

[17] A. Raj and A. Van Oudenaarden, Cell **135**, 216 (2008).
[18] G. Balázsi, A. van Oudenaarden, and J. J. Collins, Cell **144**, 910 (2011).
[19] A. D. Lander, Q. Nie, and F. Y. Wan, Dev. Cell **2**, 785 (2002).
[20] G. Hornung, B. Berkowitz, and N. Barkai, Phys. Rev. E **72**, 041916 (2005).
[21] A. Kicheva, P. Pantazis, T. Bollenbach, Y. Kalaidzidis, T. Bittig, F. Jülicher, and M. González-Gaitán, Science **315**, 521 (2007).
[22] M. B. Elowitz, A. J. Levine, E. D. Siggia, and P. S. Swain, Science **297**, 1183 (2002).
[23] M. Kærn, T. C. Elston, W. J. Blake, and J. J. Collins, Nat. Rev. Genet. **6**, 451 (2005).
[24] A. M. Arias and P. Hayward, Nat. Rev. Genet. **7**, 34 (2006).
[25] X.-D. Zheng, J. Mei, D.-H. Chen, and Y. Tao, Phys. Rev. E **98**, 042406 (2018).
[26] A. Guillemin and M. P. H. Stumpf, Phys. Biol. **18**, 011002 (2021).
[27] M. M. K. Hansen, W. Y. Wen, E. Ingerman, B. S. Razooky, C. E. Thompson, R. D. Dar, C. W. Chin, M. L. Simpson, and L. S. Weinberger, Cell **173**, 1609 (2018).
[28] K. Exelby, E. Herrera-Delgado, L. G. Perez, R. Perez-Carrasco, A. Sagner, V. Metzis, P. Sollich, and J. Briscoe, Development **148**, dev197566 (2021).
[29] N. Barkai and B. Z. Shilo, Cold Spring Harbor Perspect. Biol. **1**, a001990 (2009).
[30] M. Lagha, J. P. Bothma, and M. Levine, Trends Genet. **28**, 409 (2012).
[31] G. Chalancon, C. N. Ravarani, S. Balaji, A. Martinez-Arias, L. Aravind, R. Jothi, and M. M. Babu, Trends Genet. **28**, 221 (2012).
[32] R. Perez-Carrasco, P. Guerrero, J. Briscoe, and K. M. Page, PLoS Comput. Biol. **12**, e1005154 (2016).
[33] T. E. Saunders and M. Howard, Phys. Rev. E **80**, 041902 (2009):.
[34] B. Hu, W. Chen, W.-J. Rappel, and H. Levine, Phys. Rev. Lett. **105**, 048104 (2010).
[35] J. Cotterell and J. Sharpe, Mol. Syst. Biol. **6**, 425 (2010).
[36] A. Mugler, A. Levchenko, and I. Nemenman, Proc. Natl. Acad. Sci. USA **113**, E689 (2016).
[37] D. Ellison, A. Mugler, M. D. Brennan, S. H. Lee, R. J. Huebner, E. R. Shamir, L. A. Woo, J. Kim, P. Amar, I. Nemenman *et al.*, Proc. Natl. Acad. Sci. USA **113**, E679 (2016).
[38] S. Artavanis-Tsakonas, M. D. Rand, and R. J. Lake, Science **284**, 770 (1999).
[39] D. Sprinzak, A. Lakhanpal, L. LeBon, L. A. Santat, M. E. Fontes, G. A. Anderson, J. Garcia-Ojalvo, and M. B. Elowitz, Nature (London) **465**, 86 (2010).
[40] D. Sprinzak, A. Lakhanpal, L. LeBon, J. Garcia-Ojalvo, and M. B. Elowitz, PLoS Comput. Biol. **7**, e1002069 (2011).
[41] C. Kuyyamudi, S. N. Menon, and S. Sinha, Phys. Biol. **19**, 016001 (2022).
[42] R. Kopan and M. X. G. Ilagan, Cell **137**, 216 (2009).
[43] K. F. Sonnen and C. Y. Janda, Biochem. J. **478**, 4045 (2021).
[44] T. Erdmann, M. Howard, and P. R. ten Wolde, Phys. Rev. Lett. **103**, 258101 (2009).
[45] A. D. Lander, Cell **144**, 955 (2011).
[46] J. C. Smith, Curr. Opin. Cell Biol. **7**, 856 (1995).
[47] Y. Saka and J. C. Smith, BMC Dev. Biol. **7**, 47 (2007).
[48] H. L. Ashe and J. Briscoe, Development **133**, 385 (2006).
[49] T. R. Sokolowski, T. Erdmann, and P. R. ten Wolde, PLoS Comput. Biol. **8**, e1002654 (2012).
[50] J. Briscoe and S. Small, Development **142**, 3996 (2015).
[51] O. Barad, D. Rosin, E. Hornstein, and N. Barkai, Sci. Signal. **3**, ra51 (2010).
[52] N. G. Van Kampen, *Stochastic Processes in Physics and Chemistry* (Elsevier, Amsterdam, 1992), Vol. 1.
[53] D. J. Higham, SIAM Rev. **43**, 525 (2001).
[54] See Supplemental Material at http://link.aps.org/supplemental/10.1103/PhysRevE.107.024407 for details, as well as citations to Refs. [65,66].
[55] M. J. García-García, J. T. Eggenschwiler, T. Caspary, H. L. Alcorn, M. R. Wyler, D. Huangfu, A. S. Rakeman, J. D. Lee, E. H. Feinberg, J. R. Timmer, and K. V. Anderson, Proc. Natl. Acad. Sci. USA **102**, 5913 (2005).
[56] M. L. Dequéant and O. Pourquié, Nat. Rev. Genet. **9**, 370 (2008).
[57] J. H. Kong, L. Yang, E. Dessaud, K. Chuang, D. M. Moore, R. Rohatgi, J. Briscoe, and B. G. Novitch, Dev. Cell **33**, 373 (2015).
[58] C. Kuyyamudi, S. N. Menon, and S. Sinha, Phys. Rev. E **103**, 062409 (2021).
[59] P. C. Bressloff, *Stochastic Processes in Cell Biology*, 2nd ed. (Springer, Cham, 2021), Vol. 1.
[60] https://github.com/boyonpointe/Notch-enhanced-cell-fate-determination
[61] M. Zagorski, Y. Tabata, N. Brandenberg, M. P. Lutolf, G. Tkačik, T. Bollenbach, J. Briscoe, and A. Kicheva, Science **356**, 1379 (2017).
[62] R. Vetter and D. Iber, Nat. Commun. **13**, 1145 (2022).
[63] B. Fuß and M. Hoch, Curr. Biol. **12**, 171 (2002).
[64] M. L. Basch, R. M. Brown II, H.-I. Jen, F. Semerci, F. Depreux, R. K. Edlund, H. Zhang, C. R. Norton, T. Gridley, S. E. Cole *et al.*, eLife **5**, e19921 (2016).
[65] L. Durrieu, D. Kirrmaier, T. Schneidt, I. Kats, S. Raghavan, L. Hufnagel, T. E. Saunders, and M. Knop, Mol. Syst. Biol. **14**, e8355 (2018).
[66] V. French, M. Feast, and L. Partridge, J. Insect Physiol. **44**, 1081 (1998).